Advanced Steel Construction – Vol. 20 No. 4 (2024) 413–423
DOI:10.18057/IJASC.2024.20.4.9

WEB CRIPPLING BEHAVIOUR OF COLD-FORMED STEEL CHANNELS WEB HOLES UNDER END TWO FLANGE (ETF) LOADING

Yakup Bölükbaş *

Civil Engineering Dept., School of Engineering, Aksaray University, Aksaray, 68100, Türkiye
** (Corresponding author: E-mail: ybolukbas@aksaray.edu.tr)*

ABSTRACT

The design of the web-crippling behavior of cold-formed steel elements (CFS), which have been widely used in recent years, is essential. The concentrated loads acting on CFS members cause the section's web to crush and buckle. For this reason, it is necessary to calculate the web crippling strength correctly in the design of CFS sections. In order to observe the web-crippling behavior of CFS channel sections with holes drilled in the webs, this paper presents experimental and numerical experiments. Seven sections of the real-world system intended for End Two Flange (ETF) loading scenarios underwent testing. The tested cells were simulated by the finite element method with ABAQUS software. As a result of the numerical studies, 150 different model finite element analysis results are presented in the parametric study. In addition, the equations proposed by AISI and Eurocode 3 for the web-crippling design of CFS channel sections without web holes are analyzed. The findings of parametric investigations are compared with the design equation for sections with web holes presented by Uzzaman et al., and new coefficients are suggested for this equation. As a result of the study, the distance from the hole to the loading plate of CFS channel sections affects the section bearing capacity. Increasing the hole diameter drilled into the section web reduces the bearing capacity of the section. It is seen that h/t and N/t are more effective than R/t in the equation proposed by AISI for predicting the web-crippling strength of CFS channel sections.

ARTICLE HISTORY

Received: 7 May 2024
Revised: 14 October 2024
Accepted: 7 November 2024

KEYWORDS

Cold-formed steel;
Web crippling;
Finite element analysis;
End two-flange loading;
Web hole

1. Introduction

In recent years, there has been a significant increase in the use of Cold-Formed Steel (CFS) elements as load-bearing and supplementary structural components. These elements are favored due to their superior strength-to-weight ratio compared to conventional structural steel and advantages such as flexibility in cross-sectional design and ease of assembly. When concentrated loads or support responses are applied to Cold-Formed Steel (CFS) sections, a failure condition known as "web crippling" can occur (see Fig. 1). The effect of such concentrated loads results in the crushing and buckling of the section's web. Therefore, accurate calculation of web crippling strength is crucial in the design of CFS sections [1].

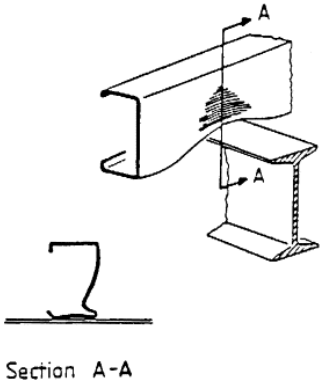

Fig. 1 Web crushing at a support point [2]

A theoretical model for predicting the web crippling capacity of Cold-Formed Steel (CFS) sections has proven challenging due to factors such as non-uniform stress distribution across the section, local yielding, significant deformations, plastic behavior in the section webs, and initial imperfections. In order to better understand this phenomenon, research has been conducted since the 1940s that have experimentally examined the web-crippling behavior of different CFS section forms [3–12]. In order to forecast the web-crippling strength of CFS sections, researchers' empirically based formulae have been integrated into the AISI [13] and AS/NZS [14] standards. While the North American standard offers a more simplified design methodology than Eurocode 3 [15], both standards' approaches are limited to specific section types and material properties.

In the following years, researchers conducted studies examining the web-crippling behavior of Cold-Formed Steel (CFS) sections for each loading condition (see Fig. 2), based on the AISI S909 [16] standard web crippling test methods [17-21].

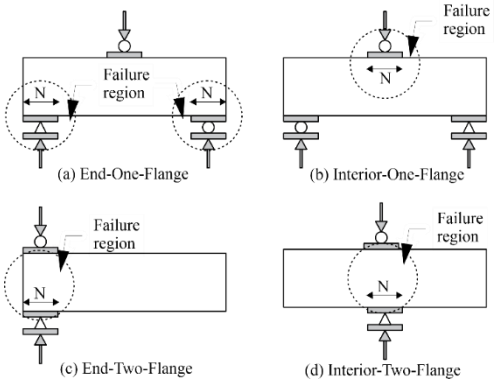

Fig. 2 Four alternative loading types for web buckling analysis [16]

In buildings composed of CFS sections, it is often necessary to create openings in the section web to install electrical or plumbing services easily. This effort is aimed at facilitating the assembly of structures. Cold-formed steel sections typically have web holes that are drilled or punched before being unstiffened. However, the portions become more vulnerable to web crippling when concentrated loads are applied close to the sites where openings are made [22].

For channel sections with holes in the web under through interior one flange (IOF) and end one flange (EOF) loading situations, Uzzaman et al. offered design ideas for web crippling strength reduction factor equations. [23-26] and Lian et al [27-30]. Furthermore, a great deal of research has been done to examine the web-crippling behavior of CFS sections that include web holes [31-36]. While the holes drilled on CFS sections are mostly drilled straight, nowadays, holes with an edge-stiffened can also be drilled. The combination of experimental and numerical investigation conducted by Uzzaman et al. on the web crippling capacity of CFS channels with edge-stiffened web holes was only documented in the literature [37–40]. They discovered that a CFS channel with edge-stiffened web holes has about the same improved web-crippling capability as a plain channel. The study by Elilarasi et al. investigates the effects of circular web openings shifted in centre or off-axis on the capacity reduction of freestanding supported lipless channels subjected to web crushing in two-end flange loading cases. Based on the results obtained from the numerical study, suitable reduction factor equations are proposed for circular web openings of lipless channels located directly under and away from the bearing plate [41]. Finally, Gunalan and Mahendran investigated the suitability of existing design rules for lipless channels subjected to web-crippling single flange loading cases and suggested appropriate adjustments where necessary [42]. In a recent study, researchers investigated the web buckling behavior of CFS channel sections

under ETF loading conditions, considering the influence of reinforced holes. Utilizing a finite element model derived from prior research, they further developed and conducted a comprehensive parametric study with this model [43]. Another finite element-based study aimed to investigate the web crippling behaviour of Sigma sections under ETF load condition. After successfully validating the numerical approach, a comprehensive numerical study was carried out on Sigma sections made of aluminium, carbon steel and stainless steel by creating 1512 numerical models. The results obtained from the numerical study were compared using parameters such as section depth, thickness, yield strength, bearing length and radius. The numerical results are also compared with the existing design equations and modified design provisions are proposed considering their inaccuracy in predicting the web crippling capacity of Sigma sections made of CF carbon steel, stainless steel and aluminium under ETF load case [44].

The CFS channel sections with web holes and their web-crippling behavior with End Two Flange (ETF) loading were investigated in this study through a battery of tests. 7 specimens were prepared with the same cross-sectional shape but with different hole sizes and locations. In addition, a finite element model of the tested specimens was created using Abaqus software [45]. The FE model was verified by comparing it with the test results. After obtaining a satisfactory FE model verification, parametric studies were carried out on 150 different models including different cross-sectional dimensions and variations of hole diameters. The equation proposed by Uzzaman et al. [24, 25] and the predictions made using the current AISI [13] and Eurocode 3 [15] standards were compared with the web crippling capacity estimates derived from the experimental and numerical research. As a result, the coefficients in the equation proposed by Uzzaman et al. [24, 25] were updated by regression analysis, and an alternative equation was proposed for the estimation of the web crippling capacity of CFS sections with web holes under ETF loading conditions.

2. Experimental study

2.1. Test specimens

This study tested 7 CFS channel sections under ETF loading conditions. While one specimen without holes in the web was tested as a reference (see Fig. 3a), six specimens were tested with web holes (see Fig. 3b). In accordance with AISI S909 [16], the length of each specimen was adjusted to be 1.5 times the web height in addition to the loading plate width for the ETF loading scenario.

The holes in the web of the specimens were drilled in two different diameters (a), 50 mm and 100 mm. The holes drilled in the web of the sections were drilled straight without any stiffening. In addition, the distances (x) of the web holes to the loading plate were adjusted as 0, 50 mm, and 150 mm. In the study, the width of the loading plate was kept constant at 50 mm. The loading plates were fixed to the top and bottom flange of the section with the help of 8 mm diameter bolts.

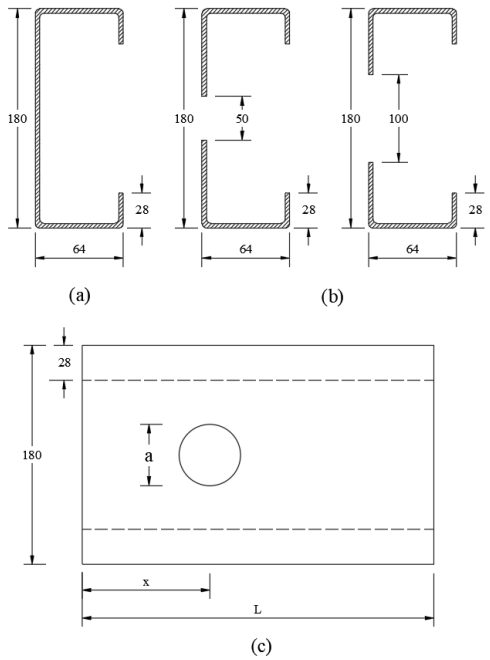

Fig. 3 Dimensions of CFS sections to be used in the study, a) reference, b) web hole specimens, c) side view of specimens (all dimensions in mm)

2.2. Specimens labelling

The labels of the test specimens are shown in Fig. 4. For example, the "ETF_Ref" identifies the reference specimen with the end of two flange loadings and no hole in the cross-sectional web. The "ETF_CIRC_50_0" indicates the model loaded with end-two flanges with a 50 mm circular hole on the web and 0 mm from the loading plate.

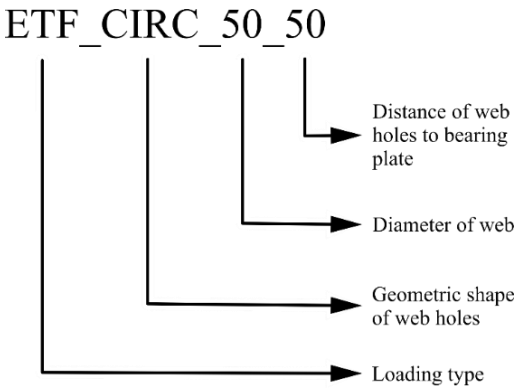

Fig. 4 Specimens labeling.

2.3. Material properties

To ascertain the mechanical characteristics of the specimens under examination, tensile tests were performed. Four coupons were prepared from flat sections of both the web and flange of the channel sections (see Fig. 5). These coupon specimens were subjected to tensile tests following EN 10002-1 [46].

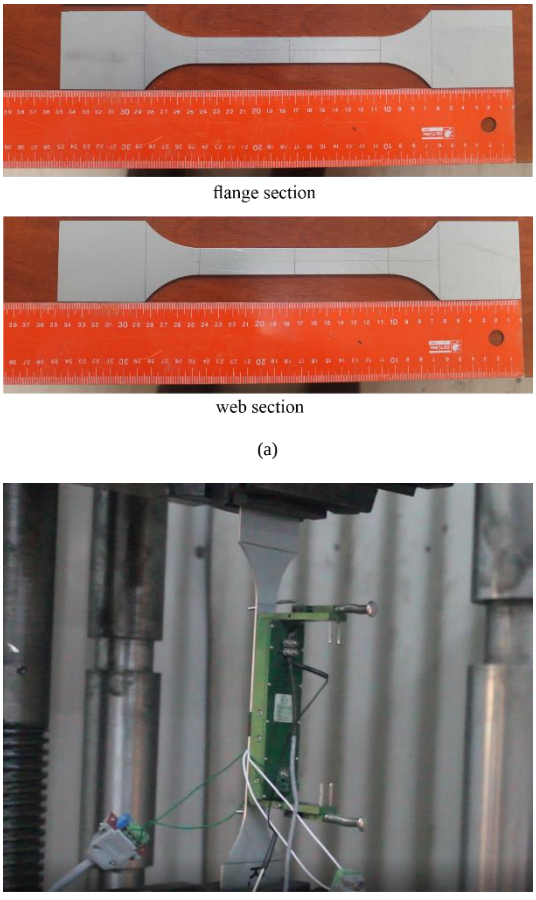

Fig. 5 Tensile test (a) Coupon specimens and (b) test setup tensile coupon test.

The engineering stress-strain curves derived from the specimens following the tensile tests are illustrated in Fig. 6. The yield strength (0.2% offset yield stress) and tensile strength of the specimens obtained from the tensile tests are presented in Table 1.

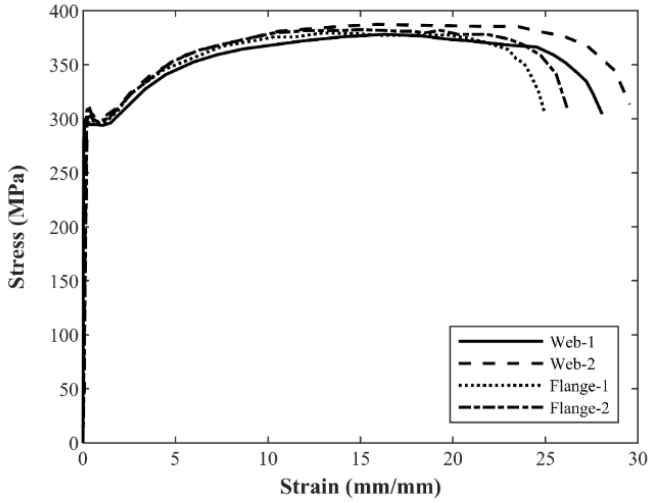

Fig. 6 Stress-strain curves

Table 1
Material properties of specimens

Specimens	σy (MPa)	σu (MPa)	εf (%)	E (MPa)
Web-1	299.75	378.13	28.066	202027
Web-2	311.78	387.33	29.55	203250
Flange-1	302.68	379.41	24.49	201768
Flange-2	308.62	380.98	26.17	205746
Mean	305.70	381.41	27.07	203197

2.4. Test rig and procedure

The prepared specimens were loaded under the ETF conditions as described in AISI S909 [16]. The loading plates were held to the top and bottom flange of the section with 8 mm diameter bolts. Semicircular joints were placed on the top of the loading plate to provide the bearing condition. Loading was applied to these semicircular joints (see Fig. 7).

A servo-controlled testing machine applied the loading to the specimen at 0.05 mm/min speed. Displacement transducers (LVDT) were used to measure displacements in the horizontal and vertical directions. Measurements were taken from the top flange to determine the vertical displacements. For horizontal displacements, measurements were taken at the center of the section under the loading plate (see Fig. 7).

During the experiment, load and displacement measurements were transferred to the data acquisition unit in such a way that 4 data can be taken per second. During the experiment, a video recording of the experiment was taken with a high-resolution camera.

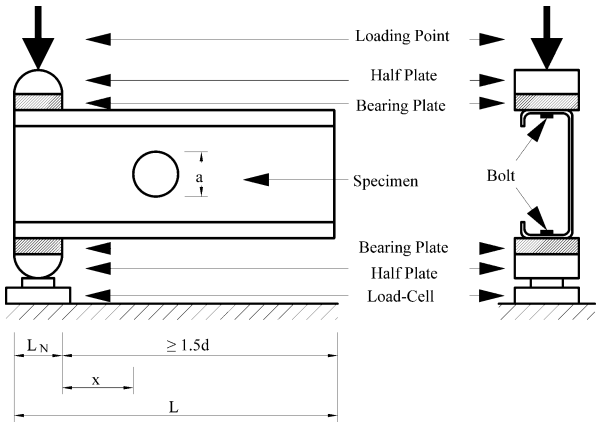

Fig. 7 Test rig

2.5. Test results

The web crippling failure loads (P_{EXP}) obtained from the experimental studies are given in Table 2. In addition, the effect of the change of the distance (x) of the holes drilled on the section web to the loading plate on the capacity is shown in Fig. 8-9. The specimens' experimental setup and failure modes are shown in Fig. 10-12.

Table 2
Web crippling capacity of specimens with circle and square web holes

Specimens	Bearing length L_N (mm)	Web hole size (mm)	Distance of web holes to the bearing plate x (mm)	Web crippling capacity P_{EXP} (kN)
ETF_REF	50	-	-	9.81
ETF_CIRC_50_0	50	50	0	9.32
ETF_CIRC_50_50	50	50	50	9.30
ETF_CIRC_50_150	50	50	150	9.93
ETF_CIRC_100_0	50	100	0	7.14
ETF_CIRC_100_50	50	100	50	8.27
ETF_CIRC_100_150	50	100	150	9.71

An analysis of Table 3 reveals that, as anticipated, the bearing capacity diminishes as the proximity of the drilled hole in the web to the bearing plate decreases. Furthermore, an increase in hole size also results in a reduction in bearing capacity. These findings are consistent with the results reported by Uzzaman et al. [24,25].

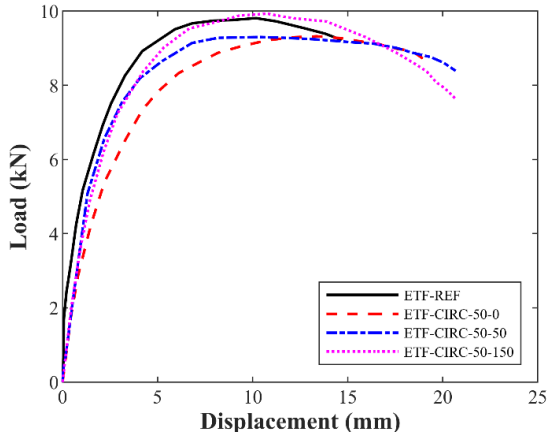

Fig. 8 The effect of hole location on web crippling capacity for 50 mm size circle hole

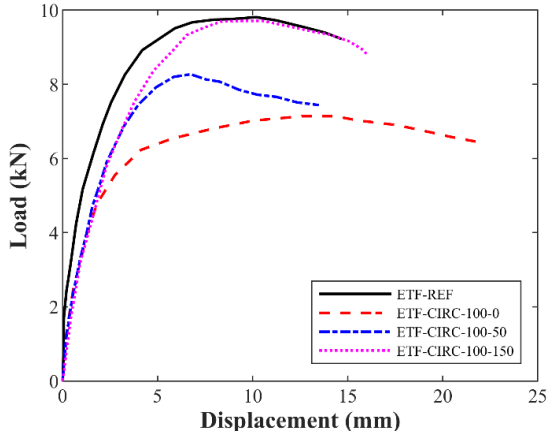

Fig. 9 The effect of hole location on web crippling capacity for 100 mm size circle hole

The bearing capacity of a CFS channel section with holes measuring 50 mm in diameter is dependent on the distance between the hole and the loading plate. The bearing capacity of the members with the hole next to the loading plate was 5% less. When the hole diameter was 100 mm, the section bearing

capacity decreased by 27%. Increasing the hole diameter reduces the capacity of the section.

Fig. 10 ETF_CIRC_50_0 specimen test setup and failure mode

Fig. 11 ETF_CIRC_50_50 specimen test setup and failure mode

Fig. 12 ETF_CIRC_50_150 specimen test setup and failure mode

3. Numerical investigation

3.1. General

In this study, a finite element (FE) model was established using ABAQUS software [41] to simulate the web-crippling behavior of Cold-Formed steel (CFS) sections under End-Two-Flange (ETF) loading conditions. The CFS channel section was meticulously transferred to the FE model to ensure precise replication of the test case, strictly following the actual dimensions. Additionally, the FE model incorporates the connections between the loading plates and the CFS section to enhance simulation fidelity.

3.2. Geometry and material properties

The cross-sectional dimensions prepared for the finite element model are shown in Fig. 3. The section dimensions used in the laboratory tests were modeled precisely in the finite element model. The loading plate was designed to be 50 mm x 80 mm.

The FE model incorporated the mechanical characteristics discovered during the tensile test. Considering the studies in the literature [24-30], the mechanical properties obtained are included in the model for the whole section, while the stress increases occurring at the corner bends and the residual stresses in the section are neglected. Engineering stress-strain behavior of the test specimens to the model, the true stress-strain curve was transferred to the model as described in the ABAQUS manual [42]. To convert the stress-strain curve obtained from the experiments to the true stress-strain curve, Eq.1 and Eq. 2.

$$\sigma_{true} = \sigma_{eng}\left(1 + \varepsilon_{eng}\right) \tag{1}$$

$$\varepsilon_{true(pl)} = \ln\left(1 + \varepsilon_{eng}\right) - \frac{\sigma_{true}}{E} \tag{2}$$

Where E is the Young's modulus, σ_{true} and ε_{true} are the true stress and strain, σ_{eng} and ε_{eng} are the engineering stress and strain.

3.3. Element type and mesh size

S4R shell element was selected in the finite element model of CFS channel sections. The S4R is a four-node double, curved, thin, or thick shell element with reduced integration and finite membrane strains. It is mentioned in the ABAQUS Manual [45] that the S4R element is suitable for complex buckling behavior. The S4R has six degrees of freedom per node and provides accurate solutions to most applications. The loading plates were modeled with the C3D8R element, which is suitable for the three-dimensional modeling of structures with plasticity, stress reinforcement, large deflection, and significant strain characteristics [45].

All sections designed in the finite element model were prepared as a 5 mm x 5 mm mesh. In the sections with web holes, it was controlled so that the dimensions of the meshes around the hole did not change too much. The mesh layout used in the finite element model is given in Fig. 13.

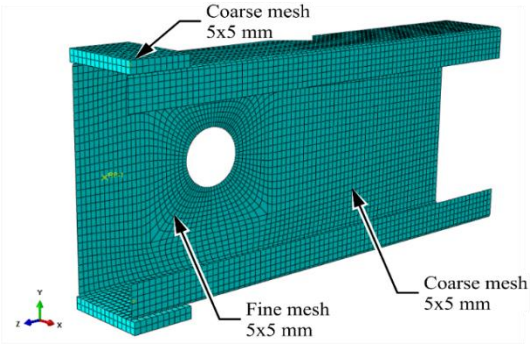

Fig. 13 Mesh type

3.4. Loading and boundary condition

The experimental study tested the CFS section in displacement with ETF loading mode. In the finite element model, loading was performed by defining a displacement of 20 mm in the y-axis perpendicular to the section flange from the loading plate connected to the CFS section top flange. Displacement in the x and z directions and rotation around the y and z axis of the upper loading flange were prevented. The displacements in the x, y, and z directions of the loading plate on the lower flange of the section were restricted, as were the rotations around the y and z axes (see Fig 14).

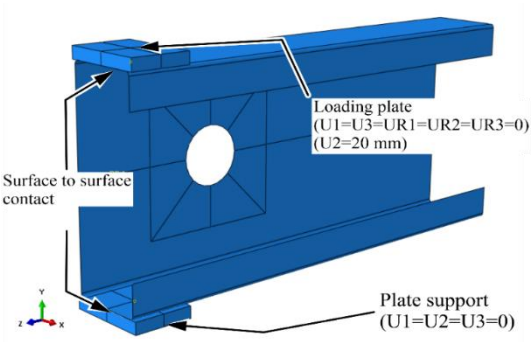

Fig. 14 Boundary conditions and contact modeling

Hard contact with friction (0.3 coefficient) is defined between the CFS section and the loading plate. This contact model describes the CFS section as slave and the loading plate as master. The CFS section head and the loading plate were fixed in laboratory experiments with 8 mm diameter bolts. This connection was simulated in the finite element model by defining a fastener element with connector properties.

3.5. Initial imperfection and residual stress

Initial geometrical imperfections and residual stresses on the section are neglected in FE models of CFS channel sections under the web crippling effect. In many studies in literature, there are analyses in which these effects are neglected [46-53]. Therefore, the initial geometrical imperfections and residual stresses on the cross-section are not considered in the FE model.

3.6. Finite element analysis performance

Finite element analysis was performed for all section types tested in laboratory studies. To demonstrate the performance of the prepared finite element model, the bearing load values (P_{FEA}) obtained as a result of the finite element analysis were compared with the load values (P_{EXP}) measured in the experimental studies. The results of this comparison are given in Table 3. The experimental load value (P_{EXP}) to the finite element analysis results (P_{FEA}) was calculated as 97%. Also, the coefficient of variation was calculated as 0.02. The comparison of the load-displacement behavior of the sections between experimental and finite element analysis is given in Fig. 15-16

Table 3
Comparison of web crippling capacity predicted from experiments and FEA

Specimens	Web crippling capacity from test P_{EXP} (kN)	Web crippling capacity from FEA P_{FEA} (kN)	Comparison P_{EXP}/P_{FEA}
ETF_REF	9.81	10.15	0.96
ETF_CIRC_50_0	9.32	9.13	1.02
ETF_CIRC_50_50	9.30	9.60	0.96
ETF_CIRC_50_150	9.93	10.17	0.97
ETF_CIRC_100_0	7.14	7.57	0.94
ETF_CIRC_100_50	8.27	8.41	0.98
ETF_CIRC_100_150	9.71	9.72	0.99
Mean			0.97
COV			0.02

As a result of the finite element analysis, the model prepared approached the experimental results by 97%. On the other hand, the COV ratio was obtained as 0.02.

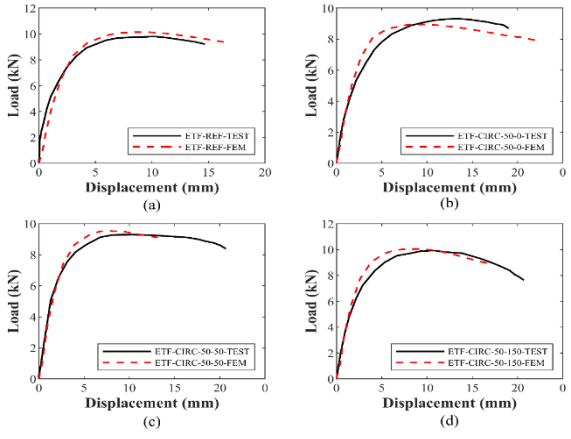

Fig. 15 Comparison between the web crippling capacity of test and FEA model

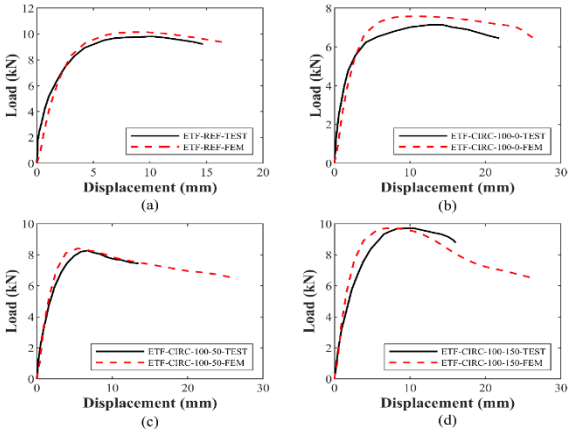

Fig. 16 Comparison between the web crippling capacity of test and FEA model

The comparison of the failure modes on the model as a result of the finite element analysis with the experimental failures is given in Fig. 17. When the pictures are examined; it is seen that in almost all sections, the failure mode result of the finite element model is consistent with the experimental collapse mode.

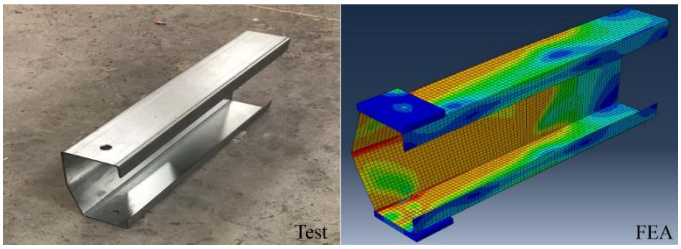

(a)

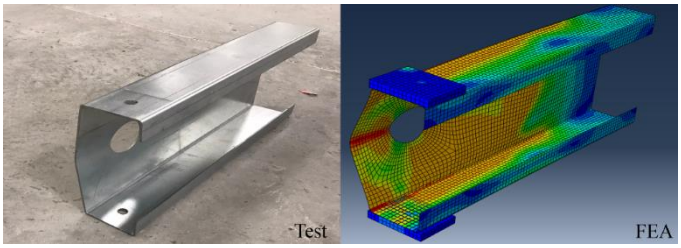

(b)

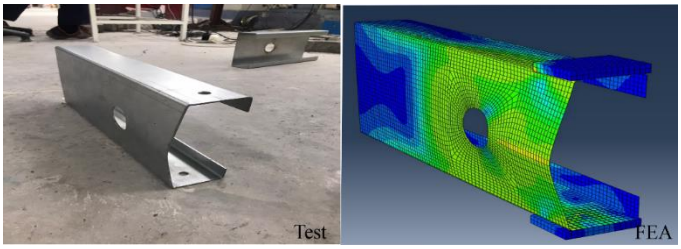

(c)

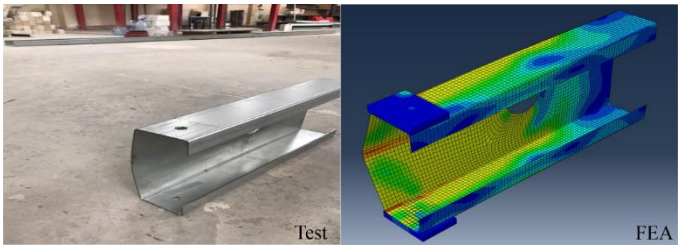

(d)

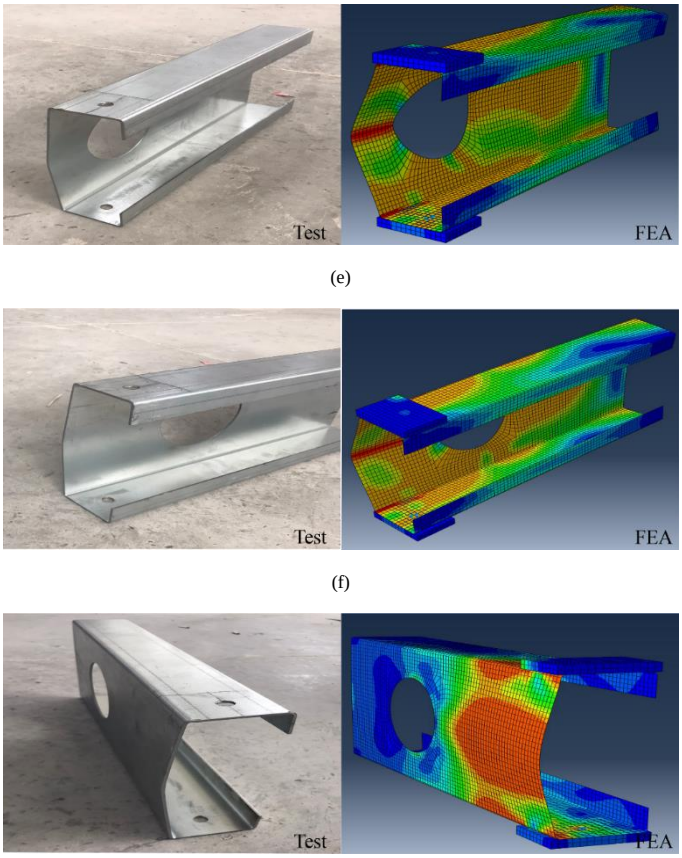

Fig. 17 Comparison between the failure modes of the test and FEA model. a) ETF_REF, b) ETF_CIRC_50_0, c) ETF_CIRC_50_50, d) ETF_CIRC_50_150, e) ETF_CIRC_100_0, f) ETF_CIRC_100_50, g) ETF_CIRC_100_150

4. Parametric study

4.1. General

After validating the FE models, a parametric study was conducted on the variation of some section parameters affecting the web-crippling capacity of these sections. In the parametric study, models without web holes were prepared, and the FE model was created to estimate the web crippling capacity. The web crippling capacity was calculated and compared with the calculation made according to the current standard AISI [13]. Similar parametric work has been done in elements with web hole. Here, according to the varying web, crippling capacities were determined by FEA and Uzzaman et al. compared with the inequality they proposed [24,25]. In all parametric studies, 150 models were created, and the section parameters affecting the web-crippling behavior of CFS channel sections were examined.

4.2. Variation of web crippling strength without holes

To investigate the web-crippling behavior of CFS channel sections, a parametric research using the finite element model with sections without web holes and with ETF loading was conducted. Considering the equation proposed in the AISI S100-16 [13] standard for the prediction of web crippling strength, the web crippling behavior is influenced by the ratio of section bend radius to thickness (R/t), web height to thickness (h/t), and loading plate width to thickness (N/t). The parametric study focuses on the effect of the variation of these three section properties on web-crippling behavior.

First, the change in web crippling capacity was analyzed by varying the web height of the CFS channel section between 50 mm and 400 mm. In comparison, the section thickness was kept constant at 2 mm, the bend diameter at 3 mm, and the loading plate width at 50 mm. The web crippling bearing capacity load obtained as a result of the parametric study is given in Table 4. In addition, the bearing capacity graph corresponding to varying web height-to-thickness (h/t) ratio is shown in Fig. 18.

Table 4
Web crippling bearing capacity load of changing h/t

Specimens	Web flat heigh (h)	Sectio thickness (t)	Section bending ra-dius (R)	Loading plate width (N)	h/t	Bearing Load (kN) (Parametric)
P1-H50	50	2	3	50	25	16.18
P1-H60	60	2	3	50	30	15.63
P1-H70	70	2	3	50	35	15.1
P1-H80	80	2	3	50	40	14.56
P1-H90	90	2	3	50	45	14.04
P1-H100	100	2	3	50	50	13.55
P1-H110	110	2	3	50	55	13.06
P1-H120	120	2	3	50	60	12.6
P1-H130	130	2	3	50	65	12.19
P1-H140	140	2	3	50	70	11.8
P1-H150	150	2	3	50	75	11.4
P1-H160	160	2	3	50	80	11.09
P1-H170	170	2	3	50	85	10.76
P1-H180	180	2	3	50	90	10.61
P1-H190	190	2	3	50	95	10.35
P1-H200	200	2	3	50	100	10.12
P1-H210	210	2	3	50	105	9.89
P1-H220	220	2	3	50	110	9.66
P1-H230	230	2	3	50	115	9.43
P1-H240	240	2	3	50	120	9.2
P1-H250	250	2	3	50	125	8.95
P1-H260	260	2	3	50	130	8.7
P1-H270	270	2	3	50	135	8.44
P1-H280	280	2	3	50	140	8.18
P1-H290	290	2	3	50	145	7.9
P1-H300	300	2	3	50	150	7.65
P1-H310	310	2	3	50	155	7.4
P1-H320	320	2	3	50	160	7.15
P1-H330	330	2	3	50	165	6.9
P1-H340	340	2	3	50	170	6.67
P1-H350	350	2	3	50	175	6.45
P1-H360	360	2	3	50	180	6.23
P1-H370	370	2	3	50	185	6.01
P1-H380	380	2	3	50	190	5.8
P1-H390	390	2	3	50	195	5.62
P1-H400	400	2	3	50	200	5.44

When Fig. 18a is examined, the h/t ratio dramatically affects the bearing capacity. The h/t increases from 25 to 200, the cross-sectional web crippling load decreases from 16 kN to 5.4 kN.

The change in capacity by changing the section height with constant section thickness, bending radius, and loading plate width on 36 different sections without holes in the web was investigated. The bearing capacity decreased by 57% with the change in section height from 50 mm to 400 mm.

In the analysis carried out to examine the effect of the width of the loading plate on the cross-sectional web crippling bearing capacity, sections with loading plate widths ranging from 20 mm to 300 mm were modeled. The thickness of the CFS channel section was kept constant at 2 mm, height 150 mm, and bend diameter 3 mm. The section length was increased for sections with large loading plate widths to meet the ETF loading case conditions. The bearing capacity obtained from the parametric study is given in Table 5. Also, the web

crippling bearing load corresponding to changing N/t is shown in Fig. 18.

Table 5
Web crippling bearing capacity load of changing N/t

Specimens	Web flat heigh (h)	Sectio thickness (t)	Section bending ra-dius (R)	Loading plate width (N)	h/t	Bearing Load (kN) (Parametric)
P2-N20	150	2	3	20	10	8.87
P2-N30	150	2	3	30	15	9.48
P2-N40	150	2	3	40	20	10.5
P2-N50	150	2	3	50	25	11.4
P2-N60	150	2	3	60	30	12.48
P2-N70	150	2	3	70	35	13.53
P2-N80	150	2	3	80	40	14.62
P2-N90	150	2	3	90	45	15.7
P2-N100	150	2	3	100	50	16.76
P2-N110	150	2	3	110	55	17.8
P2-N120	150	2	3	120	60	18.77
P2-N130	150	2	3	130	65	19.77
P2-N140	150	2	3	140	70	20.67
P2-N150	150	2	3	150	75	21.56
P2-N160	150	2	3	160	80	22.41
P2-N170	150	2	3	170	85	23.4
P2-N180	150	2	3	180	90	24.03
P2-N190	150	2	3	190	95	25.12
P2-N200	150	2	3	200	100	25.6
P2-N210	150	2	3	210	105	26.59
P2-N220	150	2	3	220	110	27.27
P2-N230	150	2	3	230	115	27.91
P2-N240	150	2	3	240	120	28.54
P2-N250	150	2	3	250	125	28.8
P2-N260	150	2	3	260	130	29.39
P2-N270	150	2	3	270	135	29.98
P2-N280	150	2	3	280	140	30.56
P2-N290	150	2	3	290	145	31.46
P2-N300	150	2	3	300	150	31.97

As the N/t increased from 10 to 150, the web crippling load increased from 8 to 32 kN. The cross-section of the loading plate width significantly affects the web's crippling strength. To determine the effect of the width of the loading plate on the bearing capacity, the parametric study examined the change in bearing capacity by varying the width of the loading plate from 20 mm to 300 mm for a section with constant web height, section thickness, and bending radius. As a result of the study, the bearing capacity increases as the loading plate width increases.

Thirty-six models were designed by varying the bending radius from 0.5mm to 5mm to investigate the effect of twist diameter-thickness (R/t) ratio on web crippling strength. Web height was kept constant at 150 mm, loading plate at 50 mm, and section thickness at 2 mm. The payloads obtained from the analysis are given in Table 6. The web crippling bearing load graph for varying R/t is shown in Fig. 18. When the graph is analyzed, the increase in the R/t caused a decrease in the section-bearing capacity.

The effect of the change of twist radius on the bearing capacity was found to be relatively less effective. Increasing the twist radius from 0.5 mm to 4 mm decreased the bearing capacity by 7%.

Table 6
Web crippling bearing capacity load of changing R/t

Specimens	Web flat heigh (h)	Sectio thickness (t)	Section bending ra-dius (R)	Loading plate width (N)	h/t	Bearing Load (kN) (Parametric)
P3-R05	150	2	0.5	50	0.25	16.28
P3-R06	150	2	0.6	50	0.3	16.13
P3-R07	150	2	0.7	50	0.35	16.04
P3-R08	150	2	0.8	50	0.4	15.82
P3-R09	150	2	0.9	50	0.45	15.76
P3-R10	150	2	1	50	0.5	15.67
P3-R11	150	2	1.1	50	0.55	15.52
P3-R12	150	2	1.2	50	0.6	15.34
P3-R13	150	2	1.3	50	0.65	15.16
P3-R14	150	2	1.4	50	0.7	14.94
P3-R15	150	2	1.5	50	0.75	14.73
P3-R16	150	2	1.6	50	0.8	14.44
P3-R17	150	2	1.7	50	0.85	14.25
P3-R18	150	2	1.8	50	0.9	14.01
P3-R19	150	2	1.9	50	0.95	13.75
P3-R20	150	2	2	50	1	13.48
P3-R21	150	2	2.1	50	1.05	13.2
P3-R22	150	2	2.2	50	1.1	12.98
P3-R23	150	2	2.3	50	1.15	12.73
P3-R24	150	2	2.4	50	1.2	12.52
P3-R25	150	2	2.5	50	1.25	12.3
P3-R26	150	2	2.6	50	1.3	12.13
P3-R27	150	2	2.7	50	1.35	11.94
P3-R28	150	2	2.8	50	1.4	11.76
P3-R29	150	2	2.9	50	1.45	11.59
P3-R30	150	2	3	50	1.5	11.43
P3-R31	150	2	3.1	50	1.55	11.29
P3-R32	150	2	3.2	50	1.6	11.13
P3-R33	150	2	3.3	50	1.65	10.95
P3-R34	150	2	3.4	50	1.7	10.83
P3-R35	150	2	3.5	50	1.75	10.7
P3-R36	150	2	3.6	50	1.8	10.57
P3-R37	150	2	3.7	50	1.85	10.44
P3-R38	150	2	3.8	50	1.9	10.32
P3-R39	150	2	3.9	50	1.95	10.23
P3-R40	150	2	4	50	2	10.15

4.3. Variation of web crippling strength with holes

An equation that computes the reduction coefficient only for the single flange loading situation has been proposed by the AISI S100-16 standard [13] for the prediction of web crippling strength of CFS channel sections with drilled holes in the web. In addition, the Eurocode standard has not made any approach in this regard. However, Uzzaman et al. [24,25], in their 2012 study, proposed an equation that calculates the web crippling strength for two flange loading cases. This equation is based on two parameters: the ratio of diameter of the web holes to the section web height (a/h) and the ratio of the loading plate to the section web height (N/h).

In this part of the parametric studies, the web crippling behavior of CFS channel sections with varying hole diameter to web height ratio (a/h) was investigated, focusing on the attenuation coefficient formula proposed by Uzzaman et al. [24,25]. The web height of the section was kept constant at 150 mm, thickness at 2 mm, bend diameter at 3 mm, and loading plate width at 50

mm. Twenty-three models were prepared by varying the hole diameter (a) between 10 mm and 120 mm. As a result of the finite element analysis, the web crippling bearing load depending on the changing a/h is given in Table 7. The comparison graph obtained from parametric study is shown in Fig. 18.

Table 7
Web crippling capacity load of changing a/h

Specimens	Web flat heigh (h)	Sectio thick-ness (t)	Section bending radius (R)	Loading plate width (N)	Hole diameter (a)	a/h	Bearing Load (kN) (Para-metric)
P4-a10	150	2	3	75	10	0.07	13.98
P4-a15	150	2	3	75	15	0.10	13.7
P4-a20	150	2	3	75	20	0.13	13.36
P4-a25	150	2	3	75	25	0.17	13.05
P4-a30	150	2	3	75	30	0.20	12.76
P4-a35	150	2	3	75	35	0.23	12.4
P4-a40	150	2	3	75	40	0.27	12.08
P4-a45	150	2	3	75	45	0.30	11.75
P4-a50	150	2	3	75	50	0.33	11.44
P4-a55	150	2	3	75	55	0.37	11.14
P4-a60	150	2	3	75	60	0.40	10.84
P4-a65	150	2	3	75	65	0.43	10.59
P4-a70	150	2	3	75	70	0.47	10.39
P4-a75	150	2	3	75	75	0.50	10.18
P4-a80	150	2	3	75	80	0.53	9.98
P4-a85	150	2	3	75	85	0.57	9.8
P4-a90	150	2	3	75	90	0.60	9.61
P4-a95	150	2	3	75	95	0.63	9.42
P4-a100	150	2	3	75	100	0.67	9.07
P4-a105	150	2	3	75	105	0.70	8.7
P4-a110	150	2	3	75	110	0.73	8.25
P4-a115	150	2	3	75	115	0.77	7.71
P4-a120	150	2	3	75	120	0.80	6.98

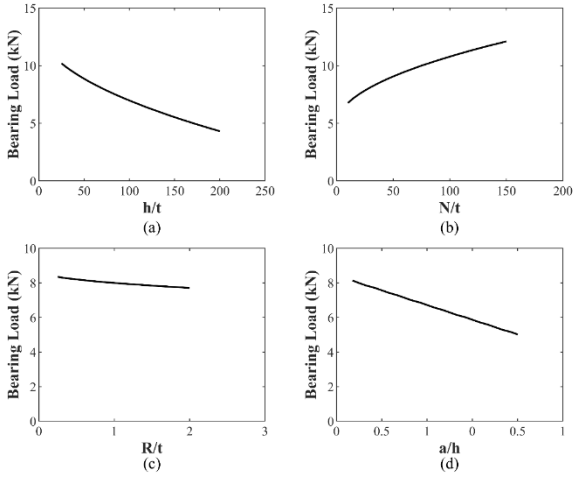

Fig. 18 Web crippling bearing the capacity load of changing parameters

When the graph is analyzed, it is seen that increasing the a/h decreases the web crippling bearing load of the CFS channel section. Although the effect of the web holes with a/h ratio of 0.2 and less is acceptable, the bearing capacity decreases significantly at higher a/h. In the parametric study on the sections with web holes, the hole diameter was varied between 10 mm and 120 mm in sections where the web height, section thickness, bending radius, and loading plate width were kept constant. The increase in hole diameter decreased the bearing capacity by 38%. In sections with web holes, the hole diameter was varied between 10 mm and 120 mm in sections where the web height, section thickness, bending radius, and loading plate width were kept constant. The increase in hole diameter decreased the bearing capacity by 38%. The Uzzaman et al. equation [24,25] uses the a/h to determine the web crippling strength of perforated CFS channel sections.

5. Current design rules

5.1. Design equations for web crippling strength of CFSS channel sections without web holes

Eurocode [15] and AISI [13] design standards are very popular for the calculation of web crippling strength of CFS sections.

5.1.1. AISI S100-16 [13]

The design equation with different coefficients according to the section shape, loading condition, and support condition can be obtained from AISI S100-16 [13]. The nominal web crippling strength ($P_{n(AISI)}$) is given in Equation 3:

$$P_{n(AISI)} = Ct^2 F_y \sin\theta \left(1 - C_R\sqrt{\frac{R}{t}}\right)\left(1 + C_N\sqrt{\frac{N}{t}}\right)\left(1 - C_h\sqrt{\frac{h}{t}}\right) \quad (3)$$

Where is the bearing length, N is the web thickness, t is the web thickness, h is the depth of the flat part of the webs, and is the inside bent radius. Fy denotes the yield stress, the angle between the web's plane and the bearing surface is represented by θ, and the coefficients of inside bent radius, bearing length, and web slenderness are represented by C_R, C_N, and C_h, respectively. Note that sections with higher r_i/t ratios are not covered by these design formulae.

5.1.2. Eurocode 3 [15]

Eurocode 3 [15] design standard provides an equation for the calculation of web crippling strength of CFS sections in ETF loading case. Unlike the AISI standard, this design, which ignores whether the flange is retained in the support state, presents a different design equation for each loading case. The following formula, based on Eurocode 3, determines the web crippling strength (Pn(EC3)) of the CFS channel segment under the ETF loading scenario.

$$P_{n(EC3)} = \frac{k_1 k_2 k_3 \left[6.66 - \frac{h_w/t}{64}\right]\left[1 + 0.01\frac{s_s}{t}\right] t^2 f_{yb}}{\gamma_{M1}} \quad (4)$$

Where, k_1, k_2, and k_3 are the coefficients from Eurocode 3; hw is the web height; t is the web thickness; ss is the nominal length of stiff bearing; f_{yb} is the basic yield stress.

5.2. Design equations for web crippling strength of CFSS channel sections with web holes

The AISI S100-16 [13] and Uzzaman et al. [24, 25] strength reduction equations were utilized to determine the web crippling strength of CFS channel sections that have web holes. The equations presented in the AISI S100-16 standard are proposed only for EOF and IOF loading cases. In Eurocode 3, there is no recommendation for the calculation of the web-crippling strength of CFS sections with holes drilled in the web.

5.2.1. AISI S100-16 [13]

To determine the web crippling strength of CFS channel sections for EOF and IOF loading drums AISI S100-16 [13] the following equations were proposed.

$$R_{c(AISI)} = 1.01 - 0.325\frac{d_h}{h} + 0.083\frac{x}{h} \leq 1.0 \quad (5)$$

$$R_{c(AISI)} = 0.90 - 0.047\frac{d_h}{h} + 0.053\frac{x}{h} \leq 1.0 \quad (6)$$

Where, d_h is the diameter of web hole; h is the depth of flat portion of web measured along the plane of web; x is the nearest distance between web hole and edge of bearing.

5.2.2. Uzzaman et al. [24,25]

Using bivariate linear regression analysis, design equations were proposed to calculate the strength reduction factor (R_p) for CFS channel sections under ITF and ETF loading. Equation 7 is proposed for unfastened flange sections in ITF loading case and Equation 8 is proposed for fastened flange. Equation 9 is proposed for unfastened flange sections in ETF loading case and Equation 10 is proposed for the fastened flange.

$$R_{p(AISI)} = 1.05 - 0.54\frac{a}{h} + 0.01\frac{N}{h} \leq 1.0 \quad (7)$$

$$R_{p(AISI)} = 1.01 - 0.051\frac{a}{h} + 0.06\frac{N}{h} \leq 1.0 \quad (8)$$

$$R_{p(AISI)} = 0.95 - 0.49\frac{a}{h} + 0.17\frac{x}{h} \leq 1.0 \quad (9)$$

$$R_{p(AISI)} = 0.96 - 0.36\frac{a}{h} + 0.14\frac{x}{h} \leq 1.0 \quad (10)$$

Where, a is the diameter of web hole; h is the depth of flat portion of web measured along the plane of web; N is the bearing length; x is the nearest distance between web hole and edge of bearing.

5.3. Proposed strength reduction factors

As shown in Table 8, the web crippling strength decreases as the size of the web holes increases. Evaluation of the experimental and numerical results shows that the a/h ratio is the primary parameter affecting the web-crippling behavior of perforated sections. Therefore, based on parametric results obtained in this study, a strength reduction factor (Rp) is proposed for the ETF loading condition using linear regression analysis.

$$R_{p(AISI)} = 0.99 - 0.58\frac{a}{h} + 0.14\frac{x}{h} \leq 1.0 \quad (11)$$

The limits for the reduction factor, given by Equation 11 are as follows: h/t ⩽156h/t⩽156, N/t⩽84N/t⩽84, N/h⩽0.63N/h⩽0.63, a/h⩽0.8a/h⩽0.8, and θ=90∘θ=90∘.

Comparison graphs were created to observe the performance of the reduction factor developed for the prediction of web buckling strength of CFS channel sections with web holes. Fig. 19 shows the variation graph of the web crippling bearing strength values predicted by the parametric study and the bearing strength values obtained by the reduction equation proposed by Uzzaman et al. [24,25] according to the a/h. In Fig. 20, the web crippling bearing strength values obtained from the parametric study are compared with the bearing strength values obtained with the reduction coefficient (Equation 11) proposed in this study.

When Fig. 19 is analyzed, the difference between the bearing capacity obtained with the reduction coefficient proposed by Uzzaman et al. [24,25] and the bearing capacity obtained in the parametric study is 8%, while the difference between the bearing capacity obtained with the reduction coefficient proposed in Equation 11 and the parametric study results is 1%.

5.4. Comparison of test results with the design strength

The results of the tests performed to determine the web crippling strength, and the prediction results of the design standards are given in Table 8. In the table, test results are compared with AISI [13], Eurocode 3 [16] and Uzzaman [24,25] predictions.

When the table is analyzed, the difference between the bearing strength values calculated according to AISI and Eurocode 3 with the reference specimen without web holes is 34% and 48%, respectively. It is seen that the design standards are more conservative in predicting the web-crippling strength of CFS channel sections without holes in the web. On the other hand, only a small number of test specimens for web portions without holes were used in this investigation. No reduction coefficient equation is advised in both AISI [13] and Eurocode 3 [16] for the prediction of the web crippling strength of CFS channel sections with web holes and ETF loading. For this reason, the reduction coefficient proposed in the studies of Uzzaman et al. [24,25] and the equations proposed in the study were used. When Table 8 is examined, it is seen that the difference between the bearing strength obtained with the reduction coefficient proposed by Uzzaman et al. [24,25] is around 4% when compared with the test results. The difference between the web crippling bearing strength values obtained with the equation proposed in the study and the results obtained in the experimental studies was 1%.

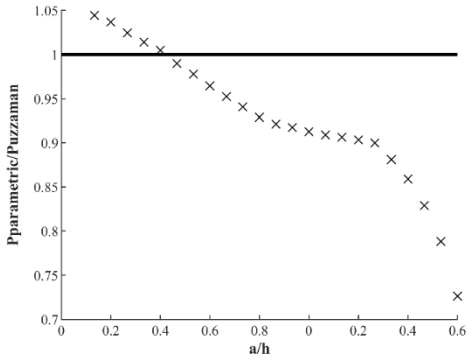

Fig. 19 Comparison between the web crippling capacity of parametric study and Uzzaman et al model

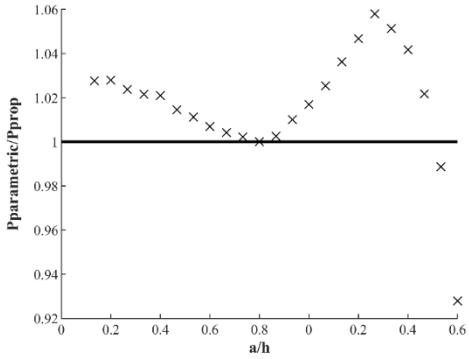

webweb

Fig. 20 Comparison between the web crippling capacity of parametric and Proposed equation model

6. Conclusions

In this study, a series of experimental and numerical studies were carried out to investigate the web-crippling behavior of CFS channel section's web holes under ETF loading. Experimental studies were carried out under ETF loading of two sections with different hole diameters. FE analysis of the test specimens was carried out with the prepared FE model. The model's performance was verified by comparing the finite element analysis with the experimental results. The web crippling strength of 150 different CFS channel sections with different cross-sectional dimensions and hole diameters was determined by the parametric study. The strengths obtained from the parametric study are compared with the equations proposed by the current AISI [13] and Eurocode [15] design standards and the equations proposed by Uzzaman et al. for the calculation of the web-crippling strength of CFS sections with cavities in the web. Finally, the coefficients of the equation proposed by Uzzaman et al. [24,25] are updated for the present problem using the linear regression method and proposed as a new equation.

- As a result of the experimental studies, it was observed that when the web holes were 50 mm in diameter, the bearing capacity decreased by about 5%, while when the hole diameter was 100 mm, the bearing capacity decreased more than expected and reached 27%.
- The variance between the bearing capacity outcomes derived from the finite element analysis and the experimental test results averaged at 3%. This discrepancy is deemed within an acceptable range for estimation.
- In the parametric study, h/t and N/t were observed as the most influential variables on the web crippling strength of CFS channel sections without holes in the web. It is seen that the a/h is an important variable in the load-carrying capacity of CFS canal sections with web holes.
- Upon comparing the bearing capacity computations derived from the prevailing design standards with the experimental test outcomes, it is evident that the AISI [13] and Eurocode 3 [15] standards exhibit conservative tendencies, showcasing differences of 34% and 48%, respectively. Additionally, an average deviation of 4% was noted between the web crippling bearing strength equation proposed by Uzzaman et al. [24,25] for sections featuring perforations in the web and the corresponding test results.
- In the context of a parametric study, the analysis of results employing the proposed equation revealed commendable predictive accuracy, with a minimal discrepancy of 1%.

Table 8
Comparison of web crippling capacity predicted from experiments, FEA and design

Specimen	Web crippling capacity (kN)						Comparison				
	P_{EXP}	P_{FEA}	P_{AISI}	P_{EC3}	$P_{Uz.}$	$P_{Prop.}$	P_{EXP}/P_{FEA}	P_{EXP}/P_{AISI}	P_{EXP}/P_{EC3}	$P_{EXP}/P_{Uz.}$	$P_{EXP}/P_{prop.}$
ETF_REF	9.81	10.15	7.31	6.63	-	-	0.96	1.34	1.48	-	-
ETF_CIRC_50_0	9.32	9.13	-	-	8.73	9.05	1.02	-	-	1.06	1.03
ETF_CIRC_50_50	9.30	9.60	-	-	9.12	9.39	0.96	-	-	1.02	0.99
ETF_CIRC_50_150	9.93	10.17	-	-	9.52	9.79	0.97	-	-	1.05	1.01
ETF_CIRC_100_0	7.14	7.57	-	-	7.71	8.05	0.94	-	-	0.93	0.89
ETF_CIRC_100_50	8.27	8.41	-	-	8.11	8.55	0.98	-	-	1.02	0.96
ETF_CIRC_100_150	9.71	9.72	-	-	8.50	8.94	0.99	-	-	1.14	1.08
Mean							**0.97**	**1.34**	**1.48**	**1.04**	**0.99**

Declaration of competing interest

The author declares that no known competing financial interests or personal relationships could have appeared to influence the work reported in this paper.

Acknowledgments

The author would like to thank Obial Silo company for supporting the CFS elements and material testing used in the studies and BABÜR DELİKTAŞ, faculty member of Bursa Uludağ University, Faculty of Engineering, Department of Civil Engineering, for his help in the finite element analysis used in the study.

References

[1] Prabakaran K. and Schuster., Web Crippling of Cold-Formed Steel Members, 14th International Specialty Conference on Cold-Formed Steel Structures (1998), 151–164.
[2] Rhodes J. and Nash D., An investigation of web crushing behavior in thin-walled beams, Thin-Walled Structures, 32, 207-230, 1998. https://doi.org/10.1016/S0263-8231(98)00035-4
[3] Winter G. and Pian R.H.J., Crushing strength of thin steel webs, Cornell Bulletin 35, Cornell University, Ithaca, N.Y., 1946.
[4] Yu W.W. and Hetrakul N., Webs for cold formed steel flexural members structural behavior of beam webs subjected to web crippling and a combination of web crippling and bending, Missouri University of Science and Technology, 1978.
[5] Bhakta B.H., LaBoube R.A. and Yu W.W., The effect of flange restraint on web crippling strength, Final Report, Civil Engineering Study, University of Missouri- Rolla, Rolla, Missouri, USA, 1992.
[6] Cain D.E, LaBoube R.A. and Yu W.W., The effect of flange restraint on web crippling strength of Cold-Formed Steel Z-and I-sections, Final Report, Civil Engineering Study, University of Missouri-Rolla, Rolla, Missouri, USA, 1995.
[7] Prabakaran K., Web Crippling of Cold-Formed Steel Sections, Project Report Department of Civil Engineering, University of Waterloo, Ontario, Canada, 1993.
[8] Prabakaran K. and Schuster B., Web crippling of cold-formed steel sections, Proc. Of 14th International Speciality Conference on Cold-Formed Steel Structures, St. Louis, Missouri, USA, 1998.
[9] Beshara B. and Schuster R.M., Web crippling of cold-formed steel C and Z sections, Proc. Of 15th International Speciality Conference on Cold-Formed Steel Structures, St.Louis, Missouri, USA, 2000.
[10] Young B. and Hancock G., Design of cold-formed channels subjected to web crippling, J. Struct. Eng., 127, 1137–1144, 2001. https://doi.org/10.1061/(ASCE)0733-9445(2001)127:10(1137)
[11] Macdonald M., Heiyantuduwa M.A., Kotelko M. and Rhodes J., Web crippling behaviour of thin-walled lipped channel beams, Thin-Walled Struct., 49, 682–690, 2011. https://doi.org/10.1016/j.tws.2010.09.010
[12] Macdonald M. and Heiyantuduwa M.A., A Design rule for web crippling of cold-formed steel lipped channel beams based on nonlinear FEA, Thin-Walled Struct., 53,123–130, 2012. https://doi.org/10.1016/j.tws.2012.01.003
[13] AISI S100-16, Specifications for the cold-formed steel structural members, cold-formed steel design manual, American Iron and Steel Institute (AISI), 2012.
[14] Standards Australia/Standards New Zealand, Australia/New Zealand Standard AS/NZS 4600 Cold-Formed Steel Structures, 2018.
[15] Eurocode. Eurocode 3: Design of steel structures - Part 1-3: General rules - Supplementary rules for cold-formed members and sheeting. European Committee for Standardization, 2007.
[16] AISI S909-17, Test Standard for Determining the Web Crippling Strength of Cold-Formed Steel Flexural Members, American Iron and Steel Institute (AISI), 2017.
[17] Sundararajah L., Mahendran M. and Keerthan P., Experimental studies of lipped channel beams subject to web crippling under two flange load cases, ASCE J. of Structural Engineering, 142(9), 04016058, 2016. https://doi.org/10.1061/(ASCE)ST.1943-541X.0001523
[18] Sundararajah L, Mahendran M. and Keerthan P., Web crippling experiments of high strength lipped channel beams under one-flange loading, J. Constr. Steel Res., 138, 851–866, 2017. https://doi.org/10.1016/j.jcsr.2017.06.011
[19] Janarthanan B., Mahendran M. and Gunalan S., Bearing capacity of cold-formed unlipped channel with restrained flanges under EOF and IOF load cases, Steel Construction Design and Research, 8 (3),146–154, 2015. https://doi.org/10.1002/stco.201510027
[20] Lian Y., Uzzaman A., Lim B.P.J., Abdelal G., Nash D. and Young B., Effect of web holes on web crippling strength of cold-formed steel channel sections under end-one-flange loading condition – Part I: tests and finite element analysis, Thin-Walled Struct., 107, 443–452, 2016. https://doi.org/10.1016/j.tws.2016.06.025
[21] Gunalan S. and Mahendran M., Web crippling tests of cold-formed steel channels under two flange load cases, J. Constr. Steel Res., 110, 1–15, 2015. https://doi.org/10.1016/j.jcsr.2015.01.018
[22] Uzzaman A., Lim B.P.J., Nash D. and Young B., Effects of edge-stiffened circular web openings on the web crippling strength of cold-formed steel channel sections under one-flange loading conditions, Eng. Struct., 139, 96–107, 2017. https://doi.org/10.1016/j.engstruct.2017.02.042
[23] Uzzaman A., Lim B.P.J., Nash D., Rhodes J. and Young B., Web crippling behaviour of cold-formed steel channel sections with offset web holes subjected to interior two-flange loading, Thin-Walled Struct., 50, 76–86, 2012. https://doi.org/10.1016/j.tws.2011.09.009
[24] Uzzaman A., Lim B.P.J., Nash D., Rhodes J. and Young B., Cold-formed steel sections with web openings subjected to web crippling under two-flange loading conditions - Part I: tests and finite element analysis, Thin-Walled Struct., 56, 38–48, 2012. https://doi.org/10.1016/j.tws.2012.03.010
[25] Uzzaman A., Lim B.P.J., Nash D., Rhodes J. and Young B., Cold-formed steel sections with web openings subjected to web crippling under two-flange loading conditions - Part II: parametric study and proposed design equations, Thin- Walled Struct., 56, 79–87, 2012. https://doi.org/10.1016/j.tws.2012.03.009
[26] Uzzaman A., Lim B.P.J., Nash D., Rhodes J. and Young B., Effect of offset web holes on web crippling strength of cold-formed steel channel sections under end-two flange loading condition, Thin-Walled Struct., 65, 34–48, 2013. https://doi.org/10.1016/j.tws.2012.12.003
[27] Lian Y., Uzzaman A., Lim J.B.P., Abdelal G., Nash D. and Young B., Effect of web holes on web crippling strength of cold-formed steel channel sections under end-one-flange loading condition - Part I: tests and finite element analysis, Thin-Walled Struct., 107, 443-452, 2016. https://doi.org/10.1016/j.tws.2016.06.025
[28] Lian Y., Uzzaman A., Lim J.B.P., Abdelal G., Nash D. and Young B., Effect of web holes on web crippling strength of cold-formed steel channel sections under end-one- flange loading condition - Part II: parametric study and proposed design equations, Thin-Walled Struct., 107, 489–501, 2016. https://doi.org/10.1016/j.tws.2016.06.026
[29] Lian Y., Uzzaman A., Lim J.B.P., Abdelal G., Nash D. and Young B., Web crippling behaviour of cold-formed steel channel sections with web holes subjected to interior-one-flange loading condition-part I: experimental and numerical investigation, Thin-Walled Struct., 111, 103–112 2017. https://doi.org/10.1016/j.tws.2016.10.024
[30] Lian Y., Uzzaman A., Lim J.B.P., Abdelal G., Nash D. and Young B., Web crippling behaviour of cold-formed steel channel sections with web holes subjected to interior-one-flange loading condition – part II: parametric study and proposed design equations, Thin-Walled Struct., 114, 92–106, 2017. https://doi.org/10.1016/j.tws.2016.10.018
[31] Yu W.W. and Davis C.S., Cold-formed steel members with perforated elements, J Struct Div 99, 2061–2077, 1973. https://doi.org/10.1061/JSDEAG.0003620
[32] Sivakumaran K.S. and Zielonka K.M., Web crippling strength of thin-walled steel members with web opening, Thin-Walled Struct., 8, 295–319, 1989. https://doi.org/10.1016/0263-8231(89)90035-9
[33] LaBoube R.A., Yu W.W., Deshmukh S.U. and Uphoff C.A., Crippling Capacity of Web Elements with Openings, J Struct Eng., 125, 137–141, 1999. https://doi.org/10.1061/(ASCE)0733-9445(1999)125:2(137)
[34] LaBoube R.A., Yu W.W. and Langan J.E., Cold-formed steel web with openings: summary report, Thin-Walled Struct., 28, 355–372, 1997. https://doi.org/10.1016/0263-8231(96)00021-3
[35] Chung K.F., Structural performance of cold formed sections with single and multiple web openings. Part-1: experimental investigation, Struct Eng., 73(9), 141-149, 1995.
[36] Chung K.F., Structural performance of cold formed sections with single and multiple web openings. Part-2: design rules. Struct Eng., 73(14), 223-228, 1995.
[37] Uzzaman A., Lim B.P.J., Nash D. and Young B., Effects of edge-stiffened circular web openings on the web crippling strength of cold-formed steel channel beams under one-flange loading conditions, Eng. Struct., 139, 96–107, 2017. https://doi.org/10.1016/j.tws.2019.106307
[38] Uzzaman A., Lim B.P.J., Nash D., Young B. and Toy K., Cold-formed steel channel beams under end-two-flange loading condition: Design for edge-stiffened holes, unstiffened holes and plain webs, Thin-Walled Struct., 147, 106532, 2020. https://doi.org/10.1016/j.tws.2019.106532
[39] Uzzaman A., Lim B.P.J., Nash D., Young B. and Toy K., Web crippling behaviour of cold-formed steel channel sections with edge-stiffened and unstiffened circular holes under interior-two-flange loading condition, Thin-Walled Struct., 154, 106813, 2020. https://doi.org/10.1016/j.tws.2020.106813.
[40] Chen B., Roy K., Fang Z., Uzzaman A., Chi Y. and Lim J.B.P., Web crippling capacity of fastened cold-formed steel channels with edge-stiffened web holes, un-stiffened web holes and plain webs under two-flange loading, Thin-Walled Struct., 163, 107666, 2021. https://doi.org/10.1016/j.tws.2021.107666
[41] Elilarasi, K., Kasthuri, S., and Janarthanan, B., Effect of circular openings on web crippling of unlipped channel sections under end-two-flange load case, Advanced Steel Construction, 16 (4), 310-320, 2020. https://doi.org/10.18057/IJASC.2020.16.4.3

[42] Gunalan, S., and Mahendran, M., Experimental study of unlipped channel beams subject to web crippling under one flange load cases, Advanced Steel Construction, 15 (2), 165-172, 2020. https://doi.org/10.18057/IJASC.2019.15.2.6

[43] Wang, W., Roy, K., Fang, Z., Ananthi, G. B. G., and Lim, J. B.., Web crippling behaviour of cold-formed steel channels with elongated un-stiffened and edge-stiffened web holes under end-two-flange loading condition, Thin-Walled Struct., 195, 111398, 2024. https://doi.org/10.1016/j.tws.2023.11139

[44] Thirunavukkarasu, K., Alsanat, H., Pologanathan, K., Gunalan, S., Gatheeshgar, P., Kanthasamy, E., and Higgins, C., Web crippling behaviour of sigma sections under end two flange loading–Numerical investigation, Structures, 59, 105765, 2024. https://doi.org/10.1016/j.istruc.2023.105765

[45] ABAQUS Analysis User's Manual-Version 6.14-2. USA: ABAQUS Inc.; 2018.

[46] TS EN ISO 6892-1. Metallic materials - Tensile testing - Part 1: Method of test at room temperature (ISO 6892-1:2019). Turkish Standards Institution; 2020.

[47] Yousefi A.M., Lim J.B.P. and Charles C.G., Cold-formed ferritic stainless steel unlipped channels with web openings subjected to web crippling under interior two-flange loading condition – Part I: Tests and finite element model validation, Thin-Walled Struct., 116, 333–341, 2017.

[48] Yousefi A.M., Lim J.B.P. and Charles C.G., Web Crippling Behavior of Unlipped Cold-Formed Ferritic Stainless Steel Channels Subject to One-Flange Loadings, J Struct Eng., 144 (8), 04018105, 2018. https://doi.org/10.1061/(ASCE)ST.1943-541X.0002118

[49] Yousefi A.M., Lim J.B.P. and Charles C.G., Web crippling strength of perforated cold-formed ferritic stainless steel unlipped channels with restrained flanges under one- flange loadings, Thin-Walled Struct., 137, 94–105, 2019. https://doi.org/10.1016/j.tws.2019.01.002

[50] Yousefi A.M., Lim J.B.P., Uzzaman, A., Uzzaman Y., Charles C.G., and Young B., Web crippling strength of cold-formed stainless steel lipped channel-sections with web openings subjected to interior-one-flange loading condition, Steel Compos Struct., 21, 629–59, 2016. https://doi.org/10.12989/scs.2016.21.3.629

[51] Fang Z., Roy K., Ma Q., Uzzaman A. and Lim J.B.P., Application of deep learning method in web crippling strength prediction of cold-formed stainless steel channel sections under end-two-flange loading, Struct., 33, 2903–2942, 2021. https://doi.org/10.1016/j.istruc.2021.05.097

[52] Fang Z., Roy K., Chi Y., Chen B. and Lim J.B.P., Finite element analysis and proposed design rules for cold-formed stainless steel channels with web holes under end-one-flange loading, Struct., 34, 2876–2899, 2021. https://doi.org/10.1016/j.istruc.2021.09.017

[53] Fang Z., Roy K., Uzzaman A. and Lim J.B.P., Numerical simulation and proposed design rules of cold-formed stainless steel channels with web holes under interior-one-flange loading, Engineering Structures 252, 113566, 2022. https://doi.org/10.1016/j.engstruct.2021.113566